

This is the accepted version of the following article:

Jesús S. Mondragón Ochoa, Abdulrahman Altin, Andreas Erbe: Comparison of cathodic delamination of poly(n-alkyl methacrylates) on iron. *Materials and Corrosion*, **68**, 1326-1332, (2017), which has been published in final form at <https://doi.org/10.1002/maco.201609289>. This article may be used for non-commercial purposes in accordance with the Wiley Self-Archiving Policy [[olabout.wiley.com/WileyCDA/Section/id-820227.html](http://olabout.wiley.com/WileyCDA/Section/id-820227.html)].

This has been published as:

Jesús S. Mondragón Ochoa, Abdulrahman Altin, Andreas Erbe: Comparison of cathodic delamination of poly(n-alkyl methacrylates) on iron. *Materials and Corrosion*, **68**, 1326-1332, (2017). DOI: 10.1002/maco.201609289

Final published version of the manuscript is available from:

<https://doi.org/10.1002/maco.201609289>

Article type: Article

## Comparison of cathodic delamination of poly(n-alkyl methacrylates) on iron

Jesús S. Mondragón Ochoa, Abdulrahman Altin, Andreas Erbe\*

*Jesús Salvador Mondragón Ochoa*

Max-Planck-Institut für Eisenforschung GmbH, Max-Planck-Str. 1, 40237 Düsseldorf, Germany

*Abdulrahman Altin*

Max-Planck-Institut für Eisenforschung GmbH, Max-Planck-Str. 1, 40237 Düsseldorf, Germany

*Andreas Erbe*

Department of Materials Science and Engineering, NTNU, Norwegian University of Science and Technology, 7491 Trondheim, Norway

Max-Planck-Institut für Eisenforschung GmbH, Max-Planck-Str. 1, 40237 Düsseldorf, Germany

E-Mail: aerbe@arcor.de

Cathodic delamination is measured on iron surfaces covered with different poly(n-alkyl methacrylates), where the alkyl is an  $n\text{-C}_n\text{H}_{2n+1}$  ( $n = 1, 4, 18$ ) group. The polymers are prepared by free radical polymerization in solution and spin coated individually on iron. The materials were characterized by infrared (IR) spectroscopy, ellipsometry, and contact angle measurements. Barrier properties in potassium chloride were obtained by electrochemical impedance spectroscopy (EIS). Artificial defects in the polymer model coatings were exposed to 1M potassium chloride as corrosive medium, and cathodic delamination was measured by a scanning Kelvin probe. The surface wettability decreases as the size of the pending alkyl group in the backbone increases. The same chemical feature shows also an effect on the cathodic delamination and on the electrochemical impedance results. Delamination is roughly

twice as fast when  $n = 1$ , compared to  $n = 4$  and  $n = 18$ . The difference in delamination rate between the latter two polymers is small.

Keywords:

Poly(methyl methacrylate), Poly(n-butyl methacrylate), Poly(n-octadecyl methacrylate), Poly(stearyl methacrylate), Cathodic Delamination, Free Radical Polymerization, Wettability, Organic coatings, Hydrophobicity

## 1 Introduction

A common way to retard corrosion of metals is to coat them with a protective barrier. Polymer-based coatings are frequently used [1–3]. The adhesion of polymers to the metal surface often relies on weak van der Waals interactions, which jeopardizes the stability of the polymer/metal interface [4]. Deadhesion of polymer coating from the metal structure in corrosive atmospheres is a common problem that ultimately leads to deterioration of the material properties. For example for steel, cathodic delamination is initiated at a defect in the coating [5]. Such failure is one of the main mechanisms of coating failure starting from a defect, and has been the subject on many scientific investigations [6–11].

A great deal of understanding has been gained using the scanning Kelvin probe (SKP) to follow the delamination front and investigate the electrochemical behaviour beneath the coating [6–8]. In cathodic delamination, a galvanic cell is formed once the polymer contains sufficient amount of water. At this point, oxygen is reduced at local cathodes beneath the coating, especially in regions containing a lot of water near the delamination front. Simultaneously, metal dissolves at local anodes in areas where delamination has already occurred. The electrochemical reaction of oxygen reduction results in the formation of hydroxide ions, i.e. leads to an increase in pH underneath the surface between the cathodically

polarized metal and the material directly above it. The high pH and the aggressive intermediates from the oxygen reduction reaction directly or indirectly cause the overlaying material to delaminate from the cathodically polarized substrate [9, 12].

In the specific case of iron, cathodic delamination has been investigated using intrinsically conductive polymers such as polyaniline [10] and polypyrrole [11]. However, mechanical strength, low processibility, solubility limitations and non-meltability have so far hindered large scale applications [13, 14]. Industrial polymers such as epoxy-based, acrylic-based, and polyurethane-based coating have also been studied [15–17]. Nevertheless, studies evaluating the cathodic delamination in function of specific polymer properties like molecular weight, molecular distribution, hydrophobicity, crystallinity, chemical composition variation in the back bone, tacticity, are rare. Moreover, cathodic delamination studies have recently focused on ion mobility. Migration, rather than diffusion has been shown to be an import process for transport along the interface [12].

In this work, the cathodic delamination rate of poly(n-alky methacrylates) has been investigated for three different polymers with different hydrophobicity. To this end, methacrylate polymers have been synthesized with an alky chain of one methyl group [poly(methyl methacrylate), PMMA], one n-butyl group [poly(butyl methacrylate), PBMA] and one octadecyl group [poly(stearyl methacrylate), PSMA]. Acrylates were chosen because of their well-characterised polymerisation kinetics, which enables a reliable synthesis of polymers without strong requirements regarding control [18,19]. The delamination results are analysed in terms of ion transport at the delamination front at the polymer / metal oxide/ metal interface.

## **2 Experimental**

### **2.1 Materials**

Iron sheets (Armco Reineisen Güte 4, purity 99.87%) were obtained from AK Steel GmbH (Düsseldorf, Germany). Methyl methacrylate (MMA, 99 %), buthyl methacrylate (BMA, 99 %), anhydrous toluene, acetone and ethanol were purchased from VWR International. 2,2'-azobis(2-methylpropionitrile) (AIBN; 98 %) and stearyl methacrylate (SMA, 98 %) were supplied by Sigma Aldrich. All chemicals were reagent grade and were used without further purification.

*Synthesis of polymethacrylates.* The monomers MMA (10 g, 0.0998 mol), BMA (10 g, 0.0703 mol) and SMA (10 g, 0.0295 mol) were loaded into separated Schlenk tubes and diluted in toluene (40 mL). The reaction mixture was degassed for one hour with a low pressure argon stream, under magnetic stirring. Subsequently, the temperature was raised to 75 °C and the AIBN (0.05 g, 0.0003 mol) was introduced into the system. The polymerization reaction was allowed to continue for 3 h; afterwards the products were precipitated in ethanol and dried at 70 °C for 24 h under vacuum.

*Pretreatment of the metal coupons.* Iron coupons (15 mm \* 20 mm \* 4 mm) we were mechanically ground with silicon carbide paper from 120 to 4000-grit, followed by polishing with silicon oxide suspension (1-2 µm) until a smooth and a mirror-like surface appearance was achieved. Polished samples were sonicated in ethanol for 15 min to remove remainders of polishing suspension, washed with copious amount of ethanol and acetone (in that order) and stored under reduced pressure until use. This type of preparation has typically yielded surfaces free of residuals from the polishing suspension.

*Deposition of the polymer model coatings.* Solutions of 10 wt.-% of PMMA, PBMA and PSMA were prepared in toluene. For preparation of the coating, a volume of 200 µl polymer solution was spin-coated onto iron at 2400 rpm for 20 s. Only in the case of PMMA two layers were deposited. Thereupon, the coated iron coupons were dried at 70 °C for 5 h.

## 2.2 Characterization methods

*Infrared spectroscopy (IR).* Iron-covered polymer samples were characterized by external infrared reflection absorption, using a Bruker Vertex 70v Fourier transform IR spectrometer (Bruker, Karlsruhe, Germany), operated under vacuum. The IR absorption spectra were recorded with a spectral resolution of  $4\text{ cm}^{-1}$  using p-polarized light at an angle of incidence of  $80^\circ$ . The spectrometer was equipped with a middle band mercury cadmium telluride detector which was cooled with liquid nitrogen 1 h before measuring. Prior to coating deposition, spectra were recorded from freshly cleaned iron samples and used as background for polymer modified coupons. The final IR spectrum was obtained averaging 250 scans.

*Ellipsometry.* Thickness of the polymer coatings was determined through ellipsometry measurements using a UV/visible ellipsometer (SE 800, Sentech Instruments) equipped with a xenon lamp light source. Data in a wavelength range of 300–800 nm at angle of incidence of  $70^\circ$  were obtained. Film thickness was computed averaging measurements of three different spots for every sample and modeling with a simple air/polymer/iron model, fixing the refractive index to 1.49 (PMMA), 1.48 (PBMA) and 1.45 (PSMA) [20]. Differences in the ellipsometric parameters were analyzed with respect to the bare polished iron substrate.

*Contact angle measurements.* Water contact angle measurements were carried out with deionized water using an OCA 30 goniometer (Dataphysics) at ambient temperature. Contact angle data were determined after a residence time of 20 s by the sessile drop method; the drop volume was fixed to  $5\ \mu\text{L}$ .

## 2.3 Electrochemical evaluation of barrier properties

Electrochemical impedance spectroscopy (EIS) was used to assess the anticorrosion properties of the coatings. The experiments were conducted using a Solatron multichannel potentiostat system (Solatron 1255B Frequency Response Analyser, Solatron Multiplexer

1281 and Solatron 1286 Electrochemical Interface) in a classical three-electrode setup. The iron coated sample, with an exposed surface area of  $0.196 \text{ cm}^2$ , was used as a working electrode. A commercial  $\text{Ag}|\text{AgCl}|3\text{M KCl}$  reference electrode (Metrohm, Filderstadt, Germany) equipped a Luggin capillary was utilized, while a platinum foil served as a counter electrode. The measurements were executed applying a sinusoidal perturbation of 10 millivolts vs. open circuit potential (OCP) in a frequency range of  $10^5 - 10^{-1} \text{ Hz}$ . The resulting spectra shown here were recorded after 4h of immersion in electrolyte (1 M KCl).

#### **2.4 Cathodic delamination experiments**

Delamination experiments were performed on a commercial scanning Kelvin probe (SKP) system from KM Soft Control (Wicinski - Wicinski GbR, Wuppertal, Germany) with a  $100 \mu\text{m}$  Nickel-Chromium tip in humid air atmosphere. The working principles of SKP are described elsewhere [7, 21–23]. Before each experiment, the Kelvin probe tip was calibrated to standard hydrogen electrode (SHE) with  $\text{Cu}/\text{CuSO}_4(\text{sat.})$ . All potentials in this work are reported vs. SHE. For cathodic delamination assessment of the polymer coatings, a coated iron sample was placed onto an iron plate and a reservoir was built around one edge of the specimen with an epoxy paste. The samples were subsequently introduced into a humid SKP chamber at 95 % relative humidity at room temperature. Afterwards, the reservoir was filled with 1 M potassium chloride electrolyte, enough to put it contact with the protected iron edge and thus initiate the cathodic delamination. For better understanding, a sketch of the setup is presented in Figure 1. Progress of the delamination front was analyzed as described elsewhere [3,9]. The first point exhibiting the potential of the intact interface was taken as the position of the delamination front.

### **3 Results and discussion**

### 3.1 Preparation of the polymers

PMMA, PBMA and PSMA were synthesized by free radical polymerization at 25 wt. % of active material and thermally activated by AIBN. A rise on the viscosity of the reacting system was evident with time, suggesting that the polymerization reaction was successful [20,24]. Polymers precipitated with ease in ethanol and white-sticky products were obtained. The conversion of monomer to polymer was computed at the end of the reactions by gravimetry, as  $0.84 \pm 0.07$ ,  $0.81 \pm 0.09$  and  $0.78 \pm 0.11$  for PMMA, PBMA and PSMA respectively. A schematic of the overall reactions is depicted in Figure 2, where R represents an alkyl substituent  $\text{CH}_3$  in case of PMMA,  $\text{n-C}_4\text{H}_9$  in case of PBMA and  $\text{n-C}_{18}\text{H}_{37}$  in case of PSMA.

In the preparation process, the polymerization time was equal for the three polymers. Consequently, similar values of conversion were obtained. In radical chain polymerization, the degree of polymerisation is essentially determined the ratio  $[\text{Monomer}] / [\text{Initiator}]^{1/2}$  [18,19]. The monomer to initiator molar concentration ratios utilized were constant in all preparations to ensure similar degrees of polymerisation for the different polymers. Hence, effects of differences in degree of polymerisation can be ruled out as the origin for the observed differences in this work.

### 3.2 Characterization of polymer model coatings

The thickness of the spin-coated layers was determined by ellipsometry as  $(950 \pm 30)$  nm,  $(670 \pm 27)$  nm and  $(850 \pm 20)$  nm for PMMA, PBMA and PSMA, respectively. Furthermore, IR spectra were acquired to examine the composition of polymers on the surface and the positions of the absorption peaks were compared to those from literature [25–29]. The spectrum of each polymer is displayed in Figure 3 [PMMA, (a); PBMA (b); PSMA, (c)]. The macromolecules possess the same functional groups; the unique difference is the size of the

alkyl moieties pending from the ester group. Due to the structural similarities the spectra are quite similar. The vibrational bands found in the spectra around  $1156\text{ cm}^{-1}$  and  $1271\text{ cm}^{-1}$  are assigned to the vibration modes of C-O present in the ester group. The peaks appearing at  $1383\text{-}1385\text{ cm}^{-1}$  correspond to the symmetric scissoring of methyl groups present in the aliphatic chain and in the head of the repeating unit. The characteristic carbonyl (C=O) stretching mode was found in range of  $1731\text{-}1740\text{ cm}^{-1}$ . In the typical range  $2849\text{-}2951\text{ cm}^{-1}$  the C-H stretching modes are found [25–29]. A significant difference in absorbance of the stretching vibration of methylene and methyl group was encountered in the spectra, as expected based on the different alkyl chain lengths of the substituents R, where PSMA shows the strongest peaks, followed by PBMA and PMMA.

To examine the hydrophobicity of the polymer model coatings, contact angle measurements were carried out. It was found that the hydrophobicity of the surface is strongly affected by the alkyl chain length in a proportional manner; as shown in the Figure 4. In detail, the contact angle  $\theta$  of pristine iron was determined as  $(52 \pm 3)^\circ$  being in with good agreement with the values reported in other works [30]. When the substrate is covered with PMMA, the wettability is reduced, and  $\theta$  shifts to higher values, namely  $(85 \pm 4)^\circ$ . Even higher are the contact angles of samples coated with PBMA and PSMA, which are  $(110 \pm 5)^\circ$  and  $(150 \pm 4)^\circ$ , respectively. For PSMA,  $\theta$  is significantly higher in comparison to the other materials, and is on the limit of the superhydrophobicity range ( $\theta \geq 150^\circ$ ). The reduction of the surface free energy in function of the alkyl chain length of poly(n-alkyl methacrylates) has been previously reported with other substrate [31]. The variations of  $\theta$  have a similar tendency to those found in this work.

### 3.3 Barrier properties

With the aim of evaluating the barrier properties of the polymers, EIS measurements were

carried out. The measured spectra are displayed in the form of Bode diagrams, namely the frequency dependence of impedance modulus  $|Z|$  and phase angle (Figure 5). For PSMA and PMMA, two regions are distinguishable, one tending from the mid to high frequency range where a capacitive behavior is observed and other tending from the mid to low frequency limit where a resistive behavior is dominant. Moreover, the phase angle drops from values close to  $90^\circ$  down to  $0^\circ$ .

With respect to PMMA and bare iron, an additional resistive domain is obvious in the high frequency region, in comparison with PSMA and PMBA. Such regime is generally referred to the electrolyte resistance between the working and reference electrodes [32, 33].

An analysis of the impedance modulus values at the lowest frequencies enables to compare the protective properties of the polymers based on the charge transfer resistance. In this regard, PSMA and PBMA possess a similar impedance modulus, being slightly higher for PBMA, and both are remarkably superior in comparison with values for PMMA. These numbers suggest that PSMA and PBMA have better barrier properties than PMMA. The low-frequency impedance modulus correlates with the hydrophobicity of the protected surface.

### 3.4 Cathodic delamination

In order to study the poly(n-alkyl methacrylate)s/metal(oxide) interfaces, SKP experiments have been performed. A reliable comparison of the cathodic delamination progression was ensured by performing simultaneous investigation of sample sets exposed to the same environmental conditions in order to avoid interferences of oxygen partial pressure and relative humidity variations. For corroding polymer covered iron, the defect potential is about  $-0.3$  to  $-0.5$  V vs. SHE [17]. This range is also in agreement with the results here. The values are determined by the open circuit potential of iron in chloride containing aqueous solutions [17]. Figure 6 depicts the recorded delamination profiles for the three investigated polymers, and in Figure 7, the progress of the delamination front was analyzed with time. In general,

two characteristic potential are observed in the SKP profiles: an interfacial potential on the non-delaminated area of the intact coating of -0.1 to 0 V exhibited in the first scan, and the defect potential ( $\sim -0.4$  V), appearing close to open circuit potential which reveals the corrosion process at the metal [9]. Between these two potential, a steeped region can be observed, which represents the position of the delamination front along the distance  $x$ . In comparison, it is obvious that the delamination front progression for PMMA is much faster compared to PBMA and PSMA. A similar trend for the determined low frequency impedance was also observed. Difficulties were encountered to detect the delamination front owing to rapidly peel-off of the coating, even when measuring at long distances and with large scan speeds. The fast deadhesion of the polymer is assigned to fast migration of electrolyte along the interface. The delamination patterned of PMMA was reproducible for four samples investigated under the same conditions. The fast delamination for PMMA correlates with the much reduced barrier properties observed by EIS. As pointed out above, differences in degree of polymerisation are unlikely the reason for the difference.

For the case of PBMA and PSMA, the delamination is much slower. During the first hour, the delamination front propagates further for PSMA. After this time, delamination progresses slower for PSMA.

It is clear that the hydrophobic character of the polymers affects cathodic delamination. Such effect can be explained in terms of thermodynamic principles of solubility. More specifically, repulsive interactions between polymer and electrolyte develop at the electrolyte/polymer interface; this phenomenon can be described by the cohesive energy density [34,35]. Based on this, it is clear that wetting a hydrophobic polymer requires more energy than wetting a hydrophilic polymer, which introduces an additional energetic cost during delamination, hence slowing down the process.

On the other hand, the typical behavior of diffusion controlled delamination kinetics was

observed, where the position of the delamination front progresses with the square root of time (Figure 7). The square root dependence may suggest that the interfacial ion mobility is rate determining [36, 37]. In accordance with the observations above, the more hydrophobic the polymer is, the more hindered is migration of solvated ions along the metal/polymer interface and water uptake.

#### 4 Conclusion

A decrease in delamination rate by the increase of the alkyl chain length of the prepared poly(n-alkyl methacrylate) coatings on iron was observed. The hydrophobicity of a coating plays a major role, especially in the early stages of the delamination of an organic coating. As along the interface, mobility of water and ions are not hindered by the hydrophobic backbone of the polymer coating, a fast delamination was observed in the case of PMMA. By increasing the chain length of the organic rest to n-butyl or n-stearyl, an overall decrease in the delamination rate was observed, and barrier properties improved.

#### *Acknowledgements*

A.A. and A.E. thank the Deutsche Forschungsgemeinschaft for financial support under grant number ER 601/3-1 and ER 601/3-2 within the Priority Program 1640 “Joining by plastic deformation”. J.S.M.O. thanks the Mexican Consejo Nacional de Ciencia y Tecnología (CONACYT) for a scholarship. The authors thank Michael Rohwerder for fruitful discussions and M. Stratmann for his continuous support.

#### 5 References

- [1] R. W. Revie, H. H. Uhlig, *Corrosion and Corrosion Control: An Introduction to Corrosion Science and Engineering*, Wiley, New Jersey, **2008**.

- [2] G. Grundmeier, S. Alda, *Encyclopedia of Electrochemistry*, vol. 4, (Eds: A. Bard, M. Stratmann, G.S. Frankel), Wiley-VCH, Weinheim, Germany, **2007**, pp. 500–666.
- [3] C. D. Fernández-Solis, A. Vimalanandan, A. Altin, J. S. Mondragón-Ochoa, K. Kreth, P. Keil, A. Erbe, in *Soft Matter Aqueous Interfaces* (Eds.: P.R. Lang, Y. Liu), Lect. Notes Phys. **2016**, 917, Springer, Cham, Switzerland, pp. 29–70.
- [4] R. Gong, S. Maclaughlin, S. Zhu, *Appl. Surf. Sci.* **2008**, 254, 6802–6809.
- [5] G. Grundmeier, A. Simões, in *Encyclopedia of Electrochemistry*, Wiley-VCH Verlag GmbH & Co. KGaA, **2007**.
- [6] A. Leng, H. Streckel, M. Stratmann, *Corros. Sci.* **1998**, 41, 579–597.
- [7] M. Stratmann, A. Leng, W. Fürbeth, H. Streckel, H. Gehmecker, K.-H. Große-Brinkhaus, *Prog. Org. Coat.* **1996**, 27, 261–267.
- [8] M. Stratmann, *Corros. Sci.* **1987**, 27, 869–872.
- [9] W. Fürbeth, M. Stratmann, *Prog. Org. Coat.* **2000**, 39, 23–29.
- [10] R. J. Holness, G. Williams, D. A. Worsley, H. N. McMurray, *J. Electrochem. Soc.* **2005**, 152, B73–B81.
- [11] G. Paliwoda-Porebska, M. Stratmann, M. Rohwerder, K. Potje-Kamloth, Y. Lu, A. Z. Pich, H. J. Adler, *Corros. Sci.* **2005**, 47, 3216–3233.
- [12] D. Iqbal, J. Rechmann, A. Sarfraz, A. Altin, G. Genchev, A. Erbe, *ACS Appl. Mater. Interfaces* **2014**, 6, 18112–18121.
- [13] T. Schauer, A. Joos, L. Dulog, C. D. Eisenbach, *Prog. Org. Coat.* **1998**, 33, 20–27.
- [14] N. S. Ilicheva, N. K. Kitaeva, V. R. Duflot, V. I. Kabanova, *Int. Sch. Res. Not.* **2012**, 2012, e320316.
- [15] R. Posner, P. E. Sundell, T. Bergman, P. Roose, M. Heylen, G. Grundmeier, P. Keil, *J. Electrochem. Soc.* **2011**, 158, C185–C193.
- [16] R. Posner, M. Santa, G. Grundmeier, *J. Electrochem. Soc.* **2011**, 158, C29–C35.

- [17] J. Wielant, R. Posner, R. Hausbrand, G. Grundmeier, H. Terryn, *Corros. Sci.* **2009**, *51*, 1664–1670.
- [18] W. F. Su, *Principles of Polymer Design and Synthesis*, Springer Berlin Heidelberg, Berlin, Heidelberg, **2013**, pp. 137–183.
- [19] S. Koltzenburg, M. Maskos, O. Nuyken, *Polymere: Synthese, Eigenschaften und Anwendungen*, Springer-Verlag, **2013**.
- [20] H. Gerrens, *Polymerisationstechnik in Ullmanns Enzyklopaedie Der Technischen Chemie*, Verlag Chemie, Weinheim, **1980**.
- [21] G. S. Frankel, M. Stratmann, M. Rohwerder, A. Michalik, B. Maier, J. Doora, M. Wicinski, *Corros. Sci.* **2007**, *49*, 2021–2036.
- [22] M. Rohwerder, F. Turcu, *Electrochimica Acta* **2007**, *53*, 290–299.
- [23] K. Wapner, G. Grundmeier, *Adv. Eng. Mater.* **2004**, *6*, 163–167.
- [24] H. U. Moritz, *Chem. Eng. Technol.* **1989**, *12*, 71–87.
- [25] R. A. Nyquist, *Interpreting Infrared, Raman, and Nuclear Magnetic Resonance Spectra*, Academic Press, San Diego, **2001**.
- [26] S. J. Mumby, J. D. Swalen, J. F. Rabolt, *Macromolecules* **1986**, *19*, 1054–1059.
- [27] A. Dazzi, A. Deniset-Besseau, P. Lasch, *Analyst* **2013**, *138*, 4191.
- [28] R. H. G. Brinkhuis, A. J. Schouten, *Macromolecules* **1991**, *24*, 1496–1504.
- [29] P. Bassan, H. J. Byrne, F. Bonnier, J. Lee, P. Dumas, P. Gardner, *Analyst* **2009**, *134*, 1586.
- [30] J. Rechmann, A. Sarfraz, A. C. Götzinger, E. Dirksen, T. J. J. Müller, A. Erbe, *Langmuir* **2015**, *31*, 7306–7316.
- [31] M. Okouchi, Y. Yamaji, K. Yamauchi, *Macromolecules* **2006**, *39*, 1156–1159.
- [32] C. Fernández-Sánchez, C. J. McNeil, K. Rawson, *TrAC, Trends Anal. Chem.* **2005**, *24*, 37–48.

- [33] G. Grundmeier, W. Schmidt, M. Stratmann, *Electrochimica Acta* **2000**, *45*, 2515–2533
- [34] B. A. Miller-Chou, J. L. Koenig, *Prog. Polym. Sci.* **2003**, *28*, 1223–1270.
- [35] D.F. Evans, H. Wennerström, *The colloidal domain*, Wiley-VCH, New York, **1999**.
- [36] A. Leng, H. Streckel, K. Hofmann, M. Stratmann, *Corros. Sci.* **1998**, *41*, 599–620.
- [37] A. Leng, H. Streckel, M. Stratmann, *Corros. Sci.* **1998**, *41*, 547–578.

Received: ((will be filled in by the editorial staff))

## Figures

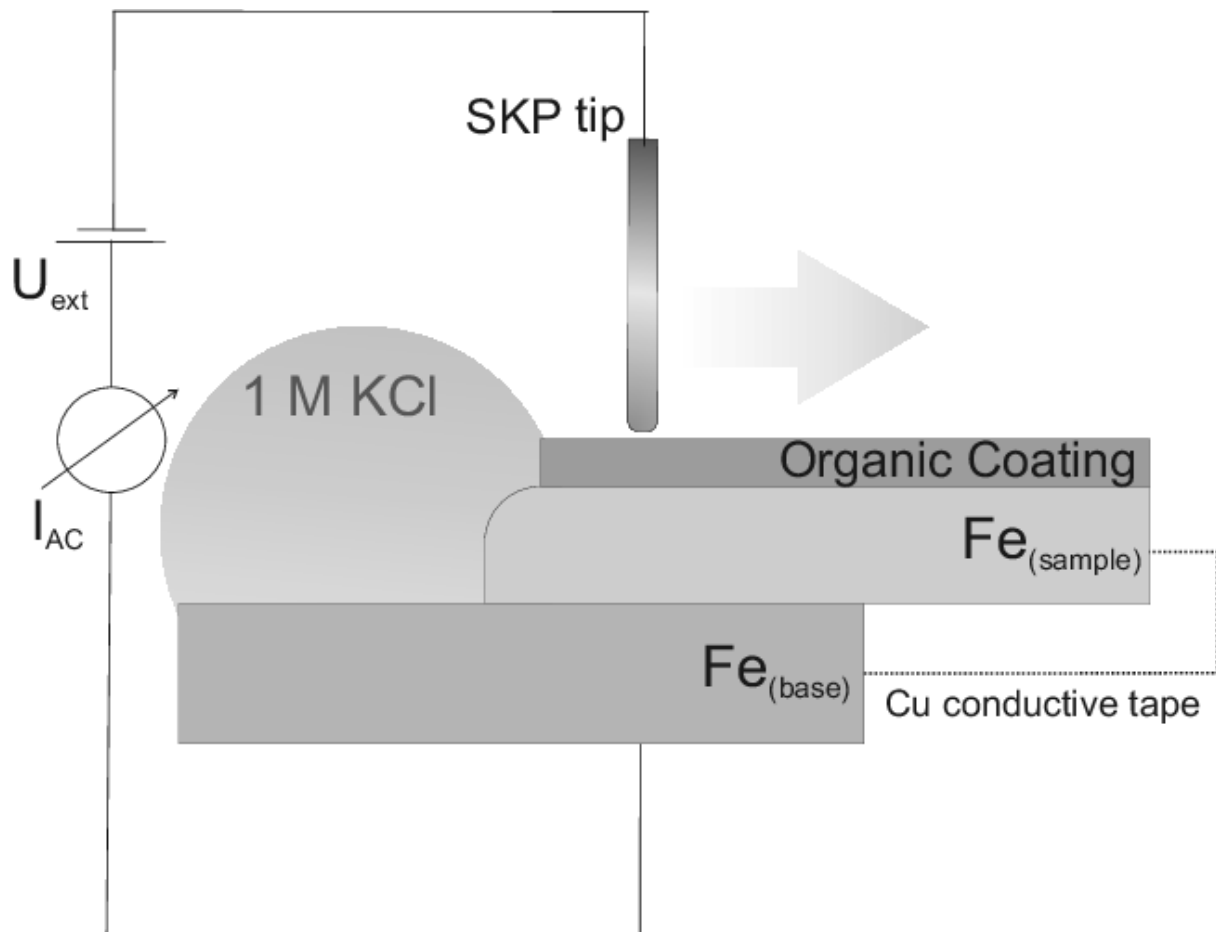


**Figure 1** Scheme depicting the delamination experiments. The arrow represents the direction of the scan.

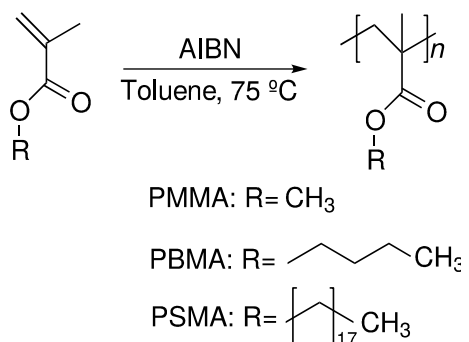


**Figure 2.** Free radical polymerization of methacrylates where R depicts the alkyl group pending in the backbone.

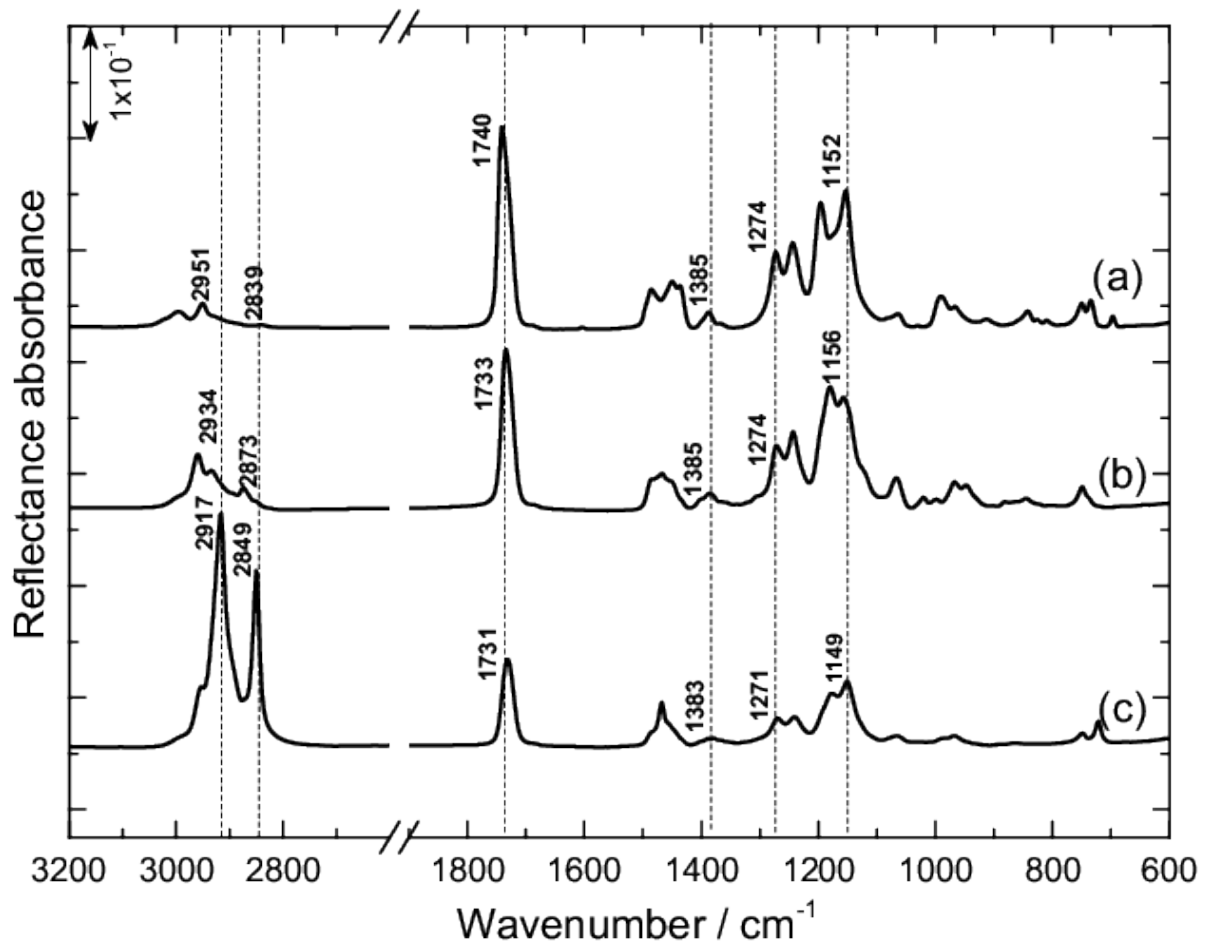


**Figure 3.** Infrared spectra of different polymer coatings deposited on iron (a) PMMA, (b) PBMA and (c) PSMA.

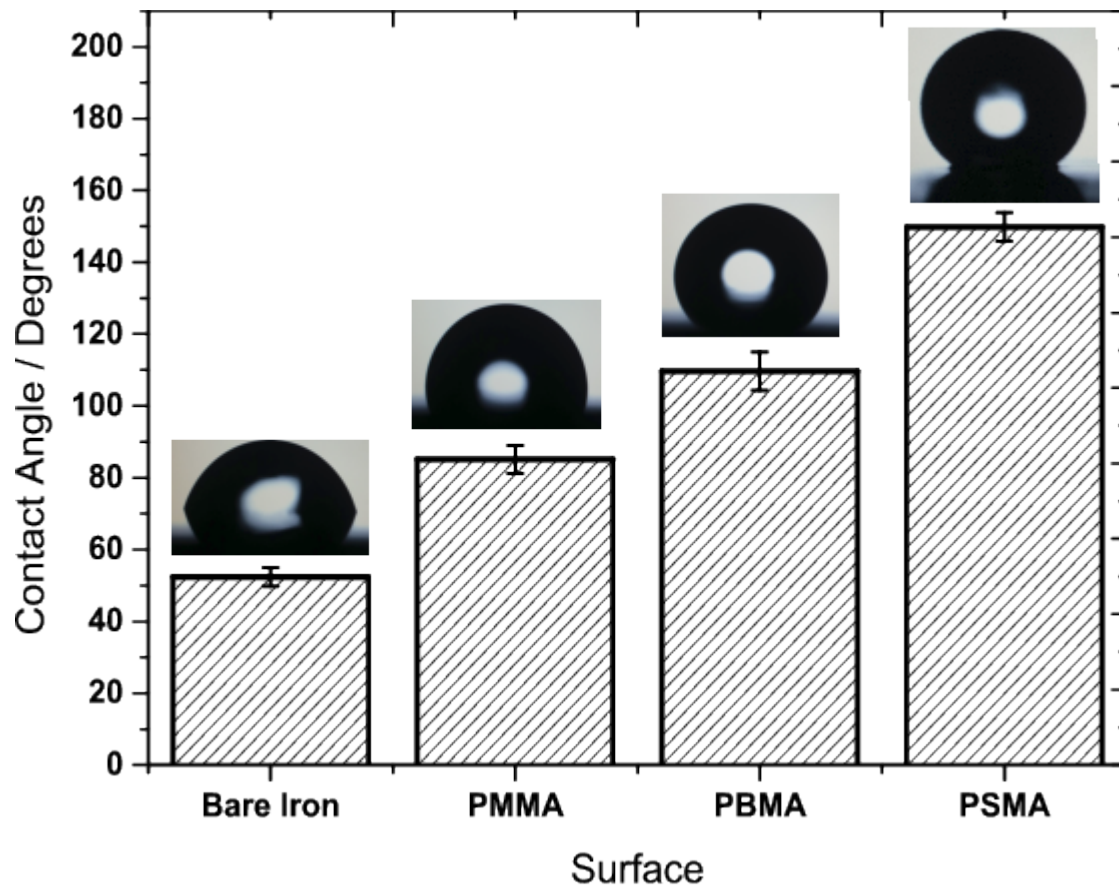


**Figure 4.** Contact angles of bare iron and the different polymers on iron. Above the bar for each surface, an image of a water drop on the respective surface is shown.

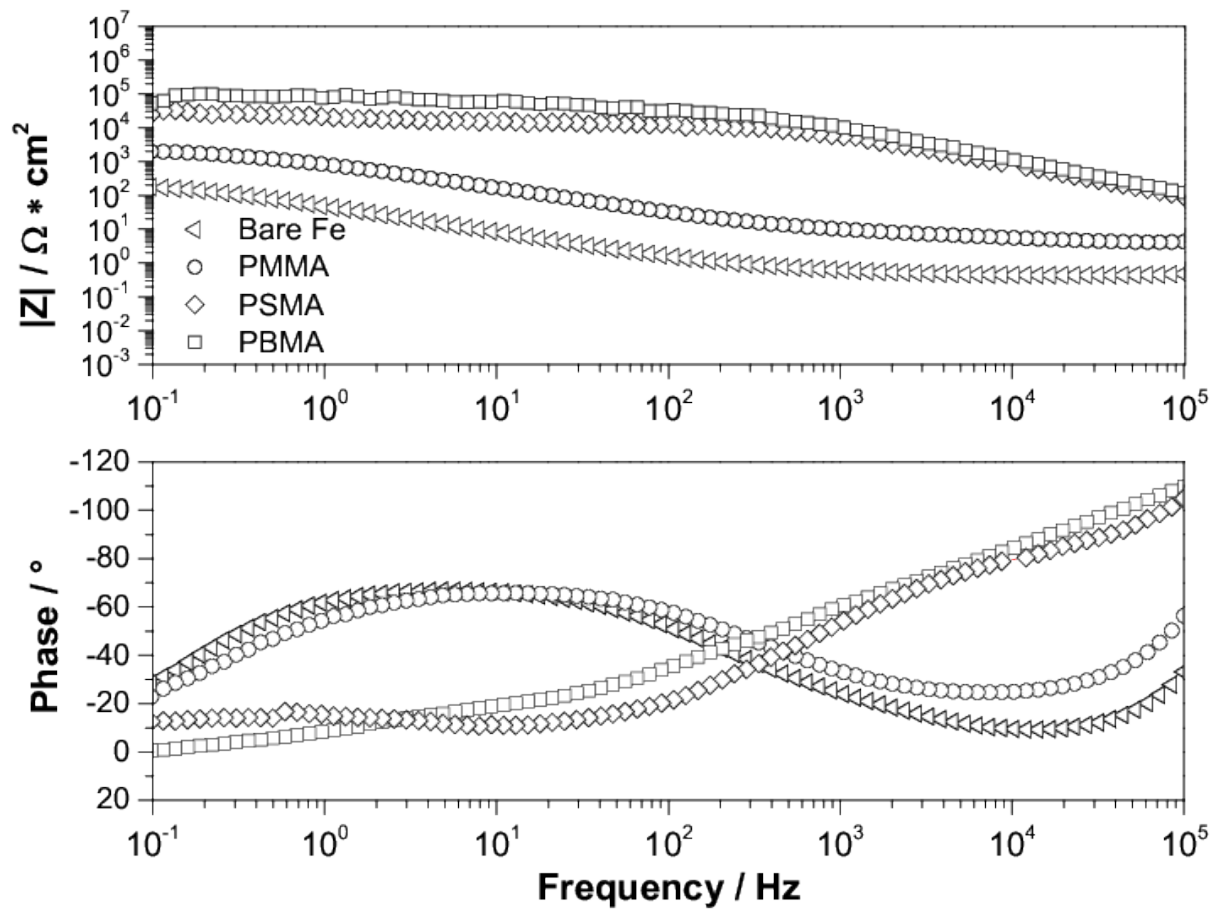


**Figure 5.** Bode plot EIS spectra of bare iron and iron coated with the synthesized polymers, recorded after 4 h of immersion in 1 M potassium chloride.

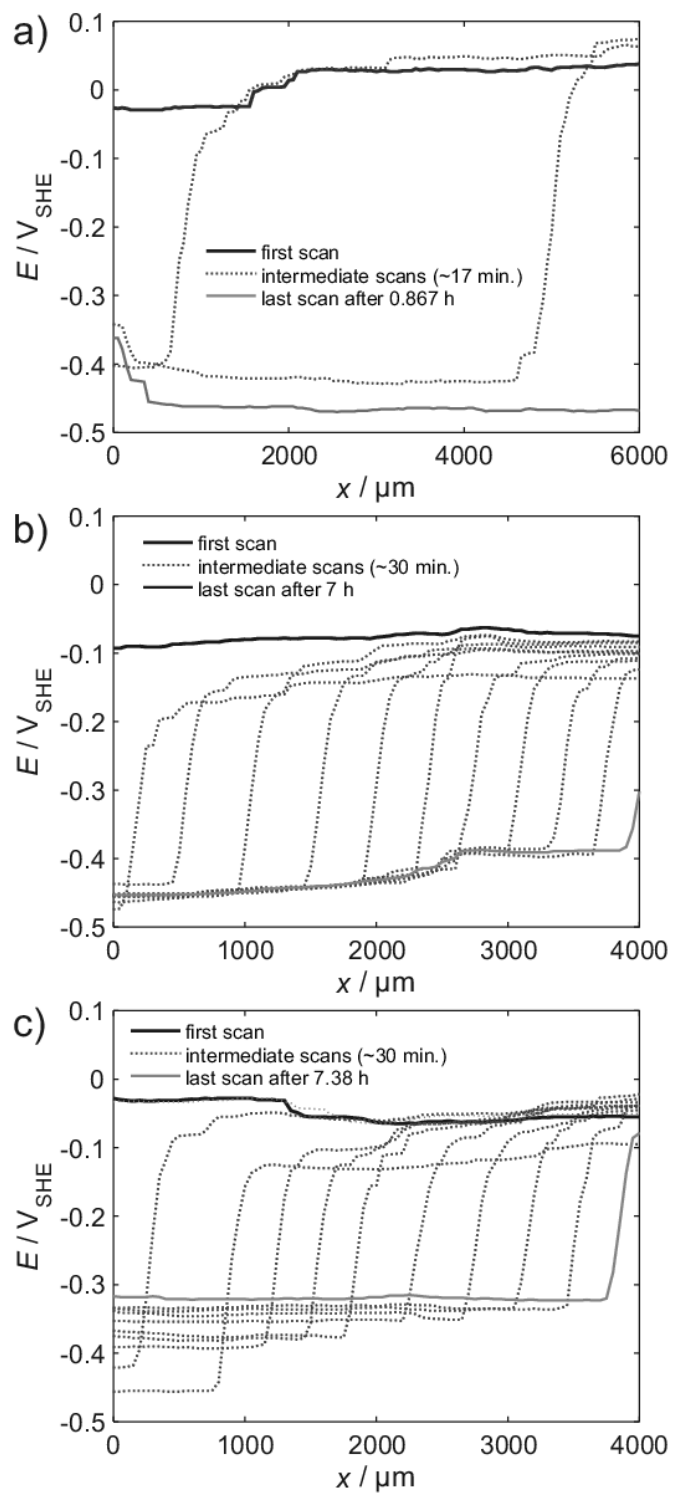


**Figure 6.** SKP delamination profiles of the a) PMMA b) PBMA and c) PSMA coatings on Fe. The experiments were executed in a setup illustrated in Figure 1, with 1 M potassium chloride in the reservoir. For a better overview not all intermediate scans in b) and c) are shown.

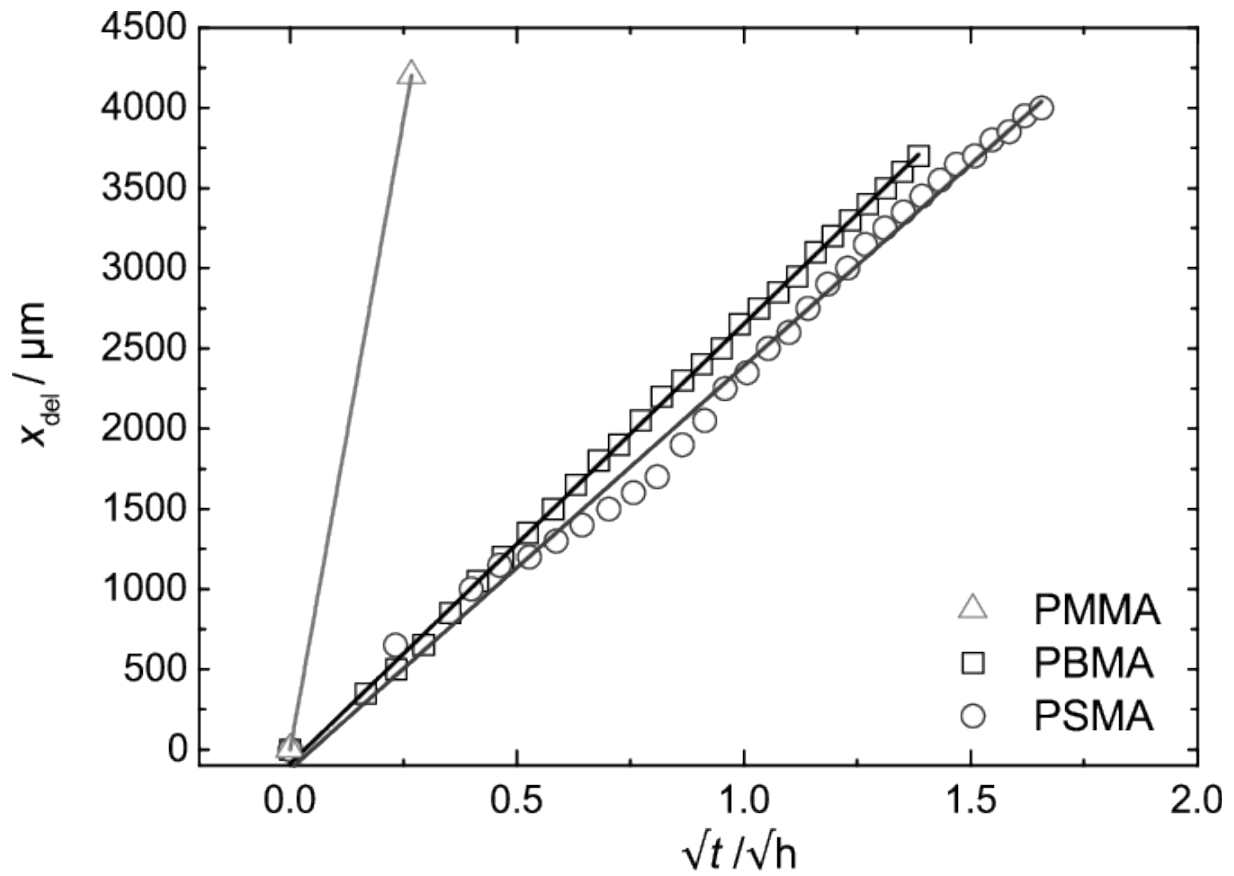


**Figure 7.** Position  $x_{\text{del}}$  of the delamination front as a function of the square root of time for different coatings applied on Fe. Extracted from the delamination curves shown in Figure 6. The start of the experiment was marked as time  $t=0$ .

**Graphical Abstract**

Cathodic delamination of poly(n-alkyl metacrylate)s-covered iron is evaluated. It is found that the n-alkyl size in the side chains of the polymers influences strongly the barrier properties of the coatings, the surface wettability as well as the delamination rate of the polymers on the metal surface in presence of a chloride-containing corrosive medium.